

Supporting Information

Suárez *et al.* 10.1073/pnas.0804597105

SI Text

Tumor Implantation and Growth *in Vivo*. LLC cells were injected intramuscularly into the calf muscle of 8-week-old VECad-Cre-ER^{T2};Dicer^{fllox/fllox} and their littermate controls (Dicer^{fllox/fllox}), previously treated or not with TMX. Mean calf diameter was determined by using a caliper as described (1). When the calf diameter reached 12–15 mm in one of the different groups the animals were killed, and the tumors were harvested. Tumors were then cut into pieces and immediately embedded and frozen in OCT compound (Tissue-Tek; Sakura). Six-micrometer frozen sections were immunostained with monoclonal anti-mouse PECAM-1 antibody to determine microvessel density.

Tumor cells were also injected s.c. into the dorsal flank of VECad-Cre-ER^{T2};Dicer^{fllox/fllox} and their littermate controls (Dicer^{fllox/fllox}), previously treated with TMX. When tumors became palpable, they were monitored for growth by measuring the length and width of the tumor using a caliper, and tumor volume was determined by the following formula: volume = 0.52 × (width)² × (length). The animals were killed, and the tumors were isolated until the tumor volume reached 5,000 mm³ in one of the different groups. Tumors were then cut into pieces and immediately embedded and frozen in OCT compound and were subsequently immunostained with monoclonal anti-mouse PECAM-1 antibody to determine microvessel density or alternatively excised into small pieces (≈2 mm × 3 mm × 1 mm) for whole-mount histology.

Mouse Hindlimb Ischemic Model and Blood Flow Assessment. After anesthesia (100 mg/kg ketamine, 10 mg/kg; xylazine) 10-week-old animals (Tie2-Cre; Dicer^{fllox/fllox} and their littermates controls Dicer^{fllox/fllox} mice) had their left femoral arteries and proximal portions of saphenous arteries exposed, ligated, and excised without damage to the femoral vein and nerve. Blood flow was measured by PeriFlux system with Laser Doppler Perfusion Module Unit (LDPU; Perimed). Deep measurement probe was placed directly on the gastrocnemius muscle to ensure a deep muscle flow measurement. Ischemic and nonischemic limb perfusion was measured before and after surgery, 1, 2, 3, and 4 weeks after surgery. The final blood flow values were expressed as the ratio of ischemic-to-nonischemic hind limb perfusion. Mice were killed at 4 weeks postsurgery and the gastrocnemius muscle was harvested, methanol-fixed, and paraffin-embedded, and 5- μ m sections were achieved for histology analysis. Semiquantitative assessment of impaired use of the ischemic limb was performed serially (3 = dragging of foot, 2 = no dragging but no plantar flexion, 1 = plantar flexion and 0 = no difference from the non ischemic hindlimb) (2). Semiquantitative measurement of the ischemic damage was also assessed (0 = no difference the nonischemic to the ischemic hind limb, 1 = mild discoloration, 2 = moderate discoloration, 3 = severe discoloration or 1–3 necrotic toes, 4 = 4–5 necrotic toes, and 5 = any loss of necrotic toes).

Wound Healing Model. Ten-week-old animals (Tie2-Cre; Dicer^{fllox/fllox} and VECad-Cre-ERT²;Dicer^{fllox/fllox} and their littermates controls Dicer^{fllox/fllox} mice) were anesthetized and two full skin punch biopsies were made with the aid of 6-mm punches (Acuderm). Wound areas were recorded one every other day and expressed as a percentage of the original wound size. At 10 days, mice were euthanized with an overdose of ketamine/xylazine and wounds were harvested with a rim of ≈2 mm of unwounded tissue. Wounds were excised, and half was used to analyze mRNA expression and

the other half was fixed in 4% PFA, paraffin-embedded, and sectioned at 5- μ m thickness for histology analysis. Semiquantitative measurement of wounding was also assessed (0 = no wound, 1 = pink skin, 2 = scub completely fallen off, 3 = scub presente, 4 = open wound).

Immunohistochemistry and Whole-Mount Analysis. Immunohistochemical staining was carried out on 6- or 5- μ m frozen or paraffin-embedded sections, respectively. PECAM-1 staining was carried out in frozen sections. Incubation with primary antibody rat anti-mouse PECAM-1, 1:200, (BD Biosciences–Pharmingen) was carried out overnight. Slides were then washed with PBS and incubated with Alexa 594–conjugated secondary antibody (Molecular Probes) for 1 h then finally coverslipped with DAPI containing mounting medium.

Paraffin sections were, where indicated, stained with hematoxylin and eosin (H&E), Massons trichrome, Sirius red, TRITC-labeled lectin (*Bandeiraea simplicifolia* 1; Sigma–Aldrich), or anti-F4/80 antibody. For F4/80 and lectin staining the sections were clarified in xylene, rehydrated, and washed with PBS. Endogenous peroxidase was inhibited with 0.3% H₂O₂ in methanol for 15 min., then washed and incubated as indicated above. Incubation with TRITC-labeled lectin (1:50) was carried out overnight, then the slides were washed with PBS and finally coverslipped with DAPI-containing mounting medium.

For whole-mount histology, tissue fragments with fairly uniform thickness (≈100 μ m) were blocked by using Fc Block (BD Biosciences) at 10 μ g/ml in 200 μ l of PBS with 1% BSA with shaking at 4°C for 10 min. After blocking, PE-labeled anti-mouse PECAM-1 antibody (BD Biosciences) was added directly to the tube and incubated for 2 h with occasional shaking at 4°C, after which samples were washed and mounted on a slide. The samples were finally viewed by fluorescence microscopy.

Fluorescent-labeled samples were visualized with a Zeiss Axiovert 2000M fluorescence microscope. Images were acquired with a CCD camera (Axio; Zeiss MicroImaging.). Analysis of different images was performed with Openlab software (Improvision) after subtracting background. Nonfluorescent samples were visualized with a Nikon Eclipse 80i light microscope coupled to a Nikon DXM 1200C digital camera.

For quantification, three to five sections per mouse sample were analyzed and from each sample two to four images were captured from random areas of each tissue section or whole-mount preparation. Microvessel density was quantified by measuring the PECAM-1 or lectin-positive structures/capillaries per sample area or per muscle fiber, respectively. Openlab software (Improvision) or ImageJ was used to determine the number of positive structures or pixels per sample area. From whole-mount preparations, microvessel area, caliber and branch points were determined by using the angiogenesis tube formation application module from MetaMorph software (Molecular Devices).

Quantitative Real-Time PCR. Total RNA was extracted from cells with TRIzol reagent (Invitrogen) according to the manufacturer's protocol. cDNA was synthesized by using Taqman RT reagents (Applied Biosystems), following the manufacturer's instructions. Quantitative real-time PCR was performed in triplicate by using the iQ SYBR Green Supermix on iCycler Real-Time Detection System (BioRad). The mRNA level was normalized by housekeeping gene 18S ribosomal RNA. The primers used for Dicer were 5'-GGA ACTAAGAGCTCAGACAG-3' (exon 20) and 5'-TTCTA-AGGAGGGTCTAGTAGC-3' (exon 21). The fold-change for

each gene from *Dicer^{flox/flox}* control cells to Tie2-Cre; *Dicer^{flox/flox}* was calculated as $2^{-\Delta\Delta C_t}$, where $\Delta\Delta C_t = \Delta C_{t\text{control}} - \Delta C_t$

Tie2-Cre; *Dicer^{flox/flox}* and where $\Delta C_t = C_{t\text{ gene of interest}} - C_{t\text{ HK gene}}$ for each condition.

1. Gerber SA, et al. (2003) Mechanism of IL-12 mediated alterations in tumor blood vessel morphology: Analysis using whole-tissue mounts. *Br J Cancer* 88:1453–1461.

2. Rutherford RB, et al. (1997) Recommended standards for reports dealing with lower extremity ischemia: Revised version. *J Vasc Surg* 26:517–538.

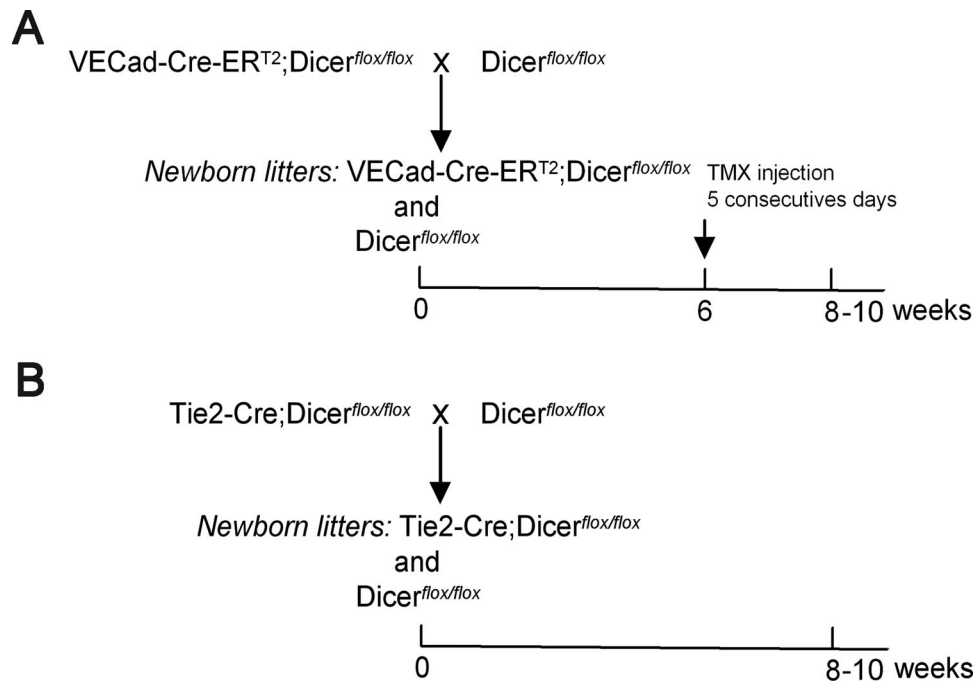


Fig. S1. Breeding strategy for experiments and TXF-induced Cre recombination. (A) Offspring from VECad-Cre-ER^{T2};Dicer^{flox/flox} mice and Dicer^{flox/flox} mice intercrossing. For the endothelial-specific and inducible deletion of *Dicer*, 6-week-old mutant mice (VECad-Cre-ER^{T2};Dicer^{flox/flox}) and their littermate controls (Dicer^{flox/flox}) were injected daily (i.p.) with 1 mg TMX. In all experiments, sex- and age-matched Dicer^{flox/flox} littermates were used. (B) Offspring from Tie2-Cre;Dicer^{flox/flox} mice and Dicer^{flox/flox} mice intercrossing. In all experiments, sex- and age-matched Dicer^{flox/flox} littermates were used.

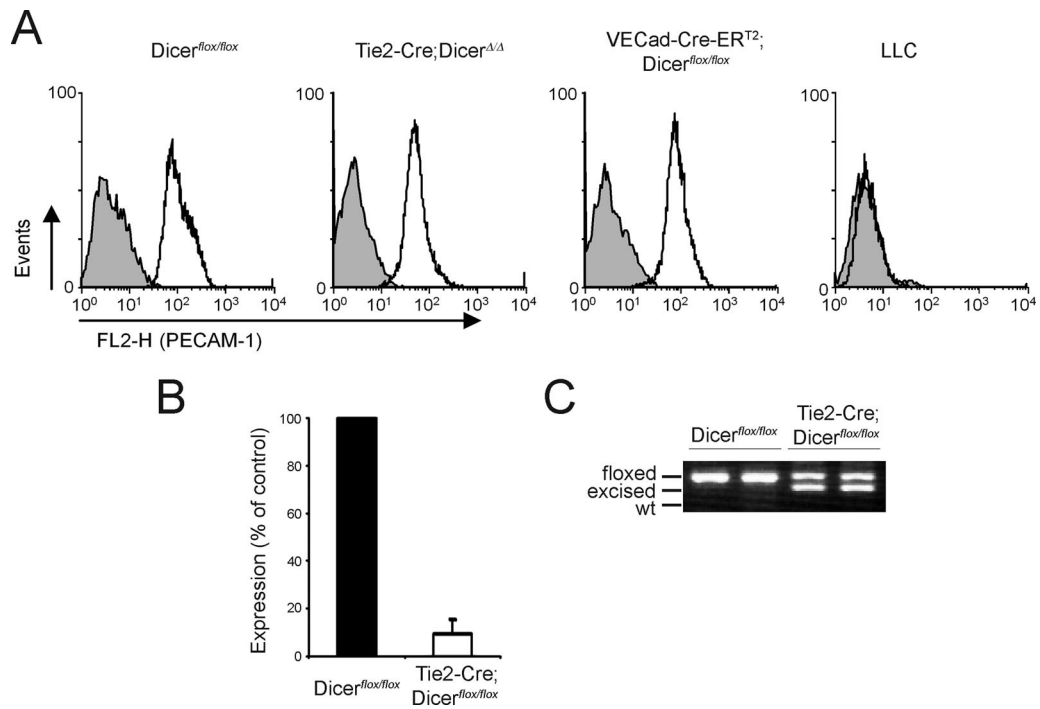


Fig. S2. Inactivation of *Dicer* in ECs. (A) ECs were isolated from the lung by immunoisolation from 3-week-old *Dicer^{flox/flox}*, *Tie2-Cre;Dicer^{flox/flox}* and *VECad-Cre-ERT²;Dicer^{flox/flox}*. After propagation cells were harvested and analyzed by FACS for PECAM-1 cell surface expression. Gray histograms represent the isotype control. LLC cells were used as negative control. (B) *Dicer* expression in MLECs from *Dicer^{flox/flox}* and *Tie2-Cre;Dicer^{flox/flox}* was analyzed by qRT-PCR. Data are expressed as percentage of control and reported as the mean \pm SD. (C) PCR genotyping and allele excision analysis of MLECs from *Dicer^{flox/flox}* and *Tie2-Cre;Dicer^{flox/flox}*.

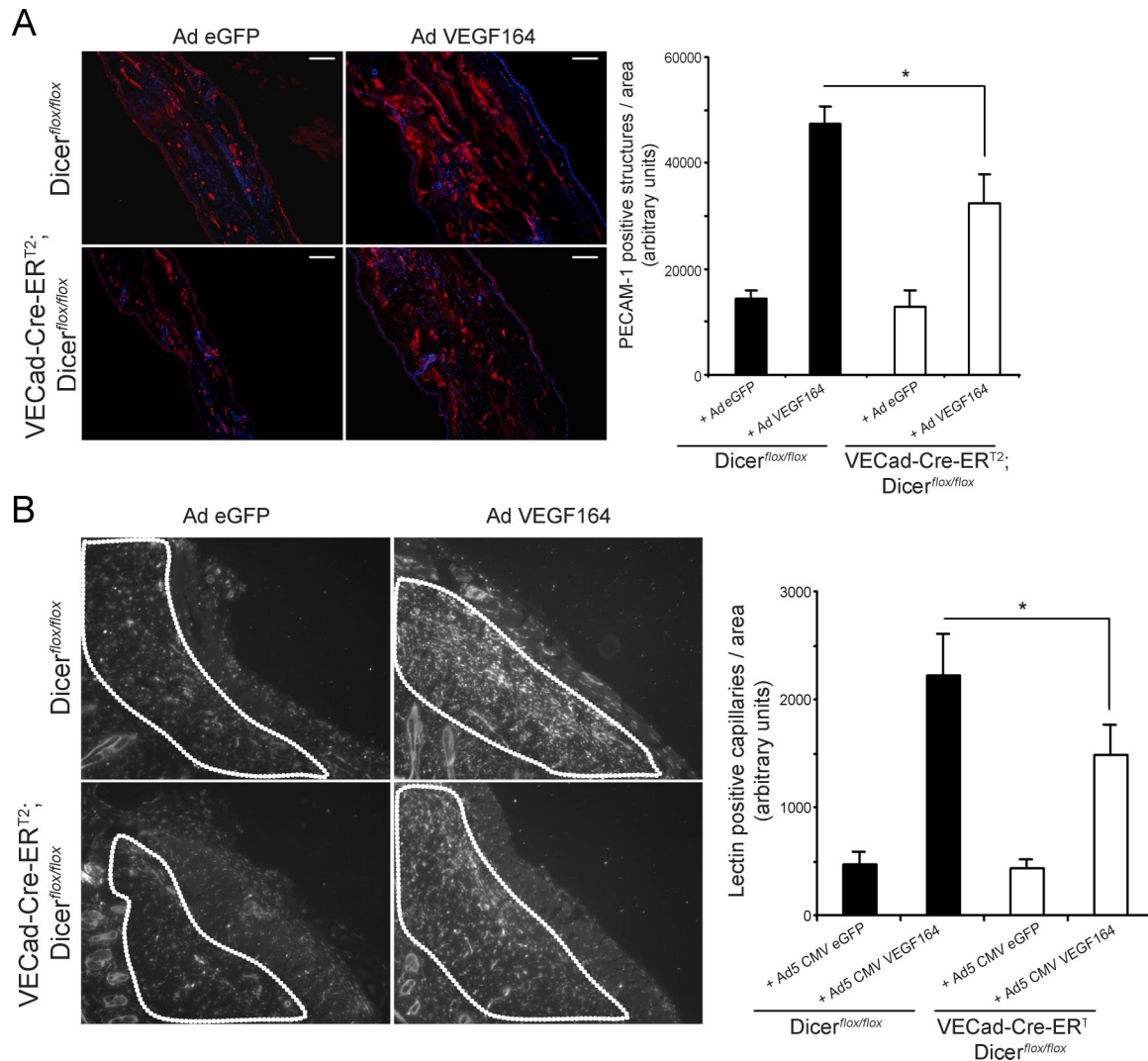


Fig. S3. Endothelial Dicer inactivation reduces VEGF-induced angiogenesis. (A) Ad-VEGF or Ad-eGFP was injected intradermally into the left and right ears, respectively of 8-week-old mice. Frozen sections were stained for PECAM-1 (red) and counterstained with DAPI (blue). Representative PECAM-1 staining showing reduced VEGF-induced angiogenesis in TMX treated VECad-Cre-ERT2;*Dicer^{flox/flox}* mice compared to *Dicer^{flox/flox}* control mice and quantification of PECAM-1 positive structures ($n = 4$ per group). (B) Ad-VEGF or Ad-eGFP was injected intradermally into the skin of the back left and right sides, respectively of 8 week-old mice. Paraffin sections were stained for lectin B4. Representative lectin binding showing reduced VEGF-induced angiogenesis in TMX treated VECad-Cre-ERT2;*Dicer^{flox/flox}*. The quantified area is indicated (between the epidermis and the muscle to avoid unspecific quantification of unspecific lectin binding to the hair follicles). Quantification of lectin positive structures ($n = 4$ per group). For each animal, 2–4 images from five sections were quantified. Values are means \pm SEM. *, $P < 0.05$, compared with *Dicer^{flox/flox}* by Student's t test. (Scale bars: A, 100 μm ; Magnification: B, $\times 20$).

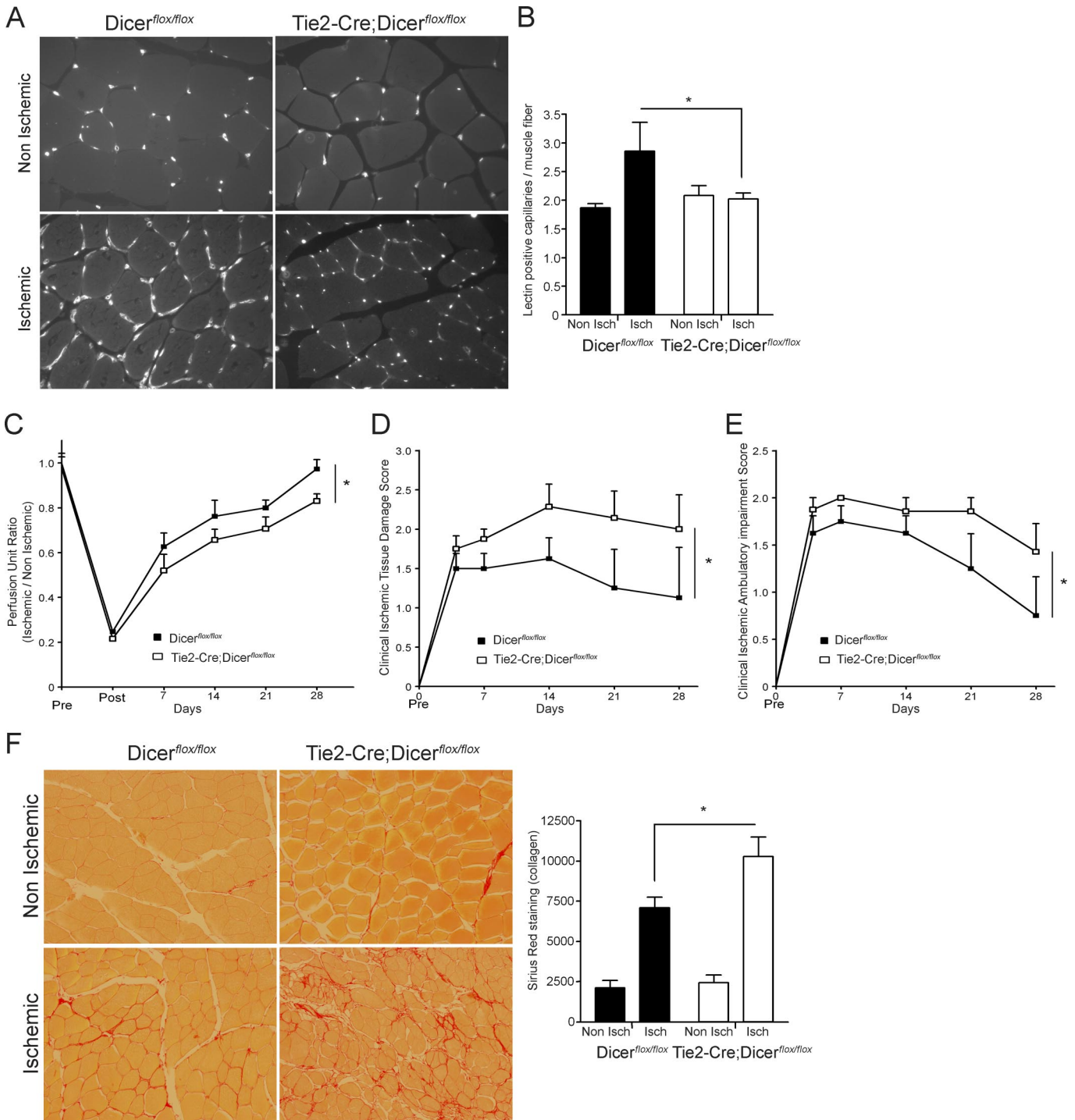


Fig. 54. Endothelial *Dicer* inactivation reduces ischemia-induced angiogenesis. (A) hindlimb ischemia was induced in 10 week-old *Dicer^{flox/flox}* or *Tie2-Cre;Dicer^{flox/flox}* mice ($n = 8$ and 7 per group, respectively). 4 weeks after surgery, postischemic angiogenesis was evaluated in gastrocnemius muscles via lectin staining. (B) Quantification of the number of capillaries per muscle fiber. For each animal, 3–5 sections were analyzed and from each sample 2–4 images were captured. $*$, $P < 0.05$, by Student's *t* test. Blood flow (C) and clinical tissue damage score (D) and ambulatory impairment score (E) was assessed over 4 weeks. Data represent mean \pm SEM. $*$, $P < 0.05$, compared with *Dicer^{flox/flox}* and *VECad-Cre-ERT²;Dicer^{flox/flox}* by two-way ANOVA. (F) Ischemic and non-ischemic gastrocnemius muscles were stained with Sirius red for collagen. Quantification of fibrosis in sections from the gastrocnemius muscles from *Dicer^{flox/flox}* and *Tie2-Cre;Dicer^{flox/flox}*. Values are means \pm SEM. $*$, $P < 0.05$, compared with *Dicer^{flox/flox}* by Student's *t* test. (Magnifications: A and F, $\times 40$ and $\times 20$, respectively).

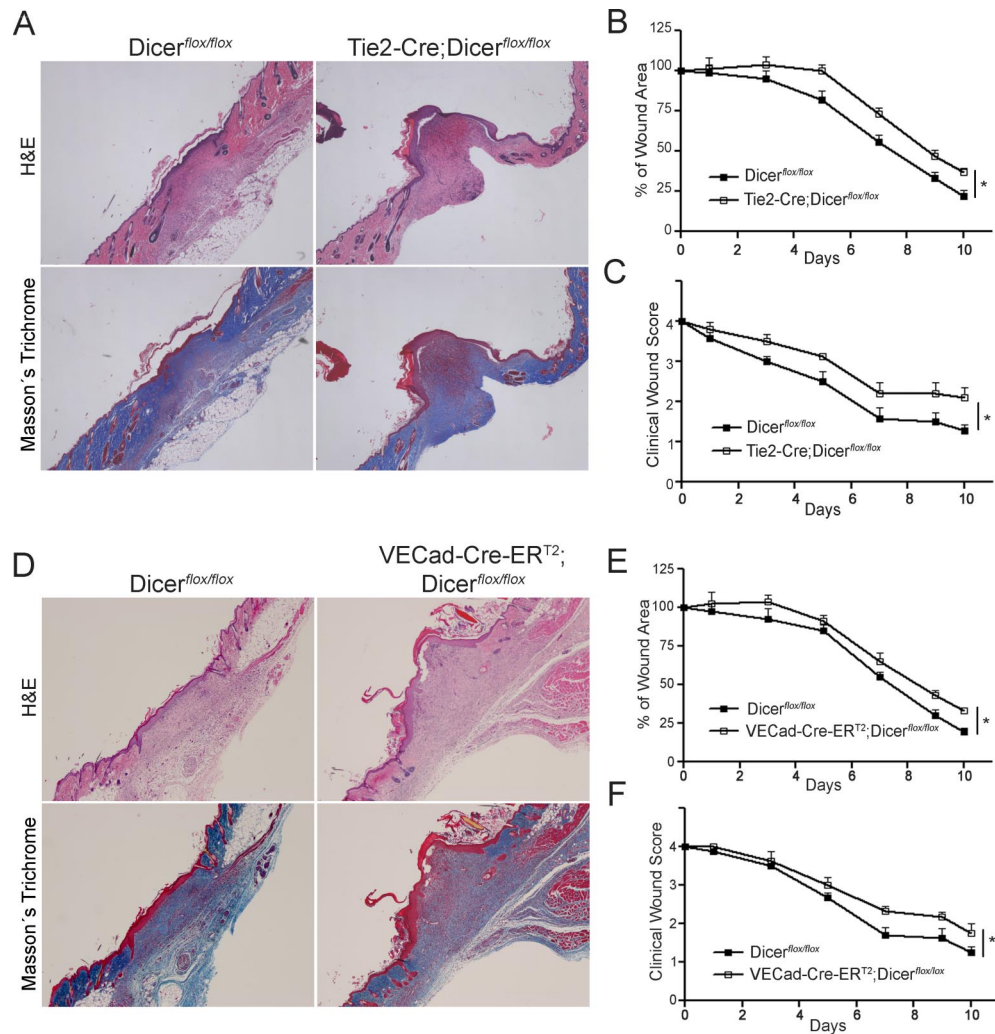


Fig. S5. Delayed wound healing in Tie2-Cre;Dicer^{flox/flox} and VECad-Cre-ER^{T2};Dicer^{flox/flox}. Two punch wounds were created on the back of 10 weeks-old Dicer^{flox/flox} or Tie2-Cre;Dicer^{flox/flox} mice (A, B, and C) or of the back of 10 weeks-old Dicer^{flox/flox} or VECad-Cre-ER^{T2};Dicer^{flox/flox} and mice previously pretreated with TMX (D, E, and F). Histological comparison of wounds from Dicer^{flox/flox} and Tie2-Cre;Dicer^{flox/flox} mice (A) or Dicer^{flox/flox} and VECad-Cre-ER^{T2};Dicer^{flox/flox} mice (D). Wounds at day 10 after wounding: wounds were stained with H&E and Masson's Trichrome as indicated. In both cases wounds from control mice exhibited smaller areas of granulation tissue devoid of hair follicles with less granulation tissue deposition and collagen accumulation, and showed early histological evidence wounding. Wound areas were measured (B and E) and clinical wound score calculated (C and F) from days 0 to 10 in control Dicer^{flox/flox} and Tie2-Cre;Dicer^{flox/flox} mice ($n = 5$ per group) (B and C, respectively) or in Dicer^{flox/flox} and VECad-Cre-ER^{T2};Dicer^{flox/flox} mice pretreated with TMX ($n = 5$ per group) (E and F, respectively). Data represent mean \pm SEM. *, $P < 0.05$, compared with Dicer^{flox/flox} and Tie2-Cre;Dicer^{flox/flox} or VECad-Cre-ER^{T2};Dicer^{flox/flox} by two-way ANOVA. (Magnification: A and D, $\times 4$).

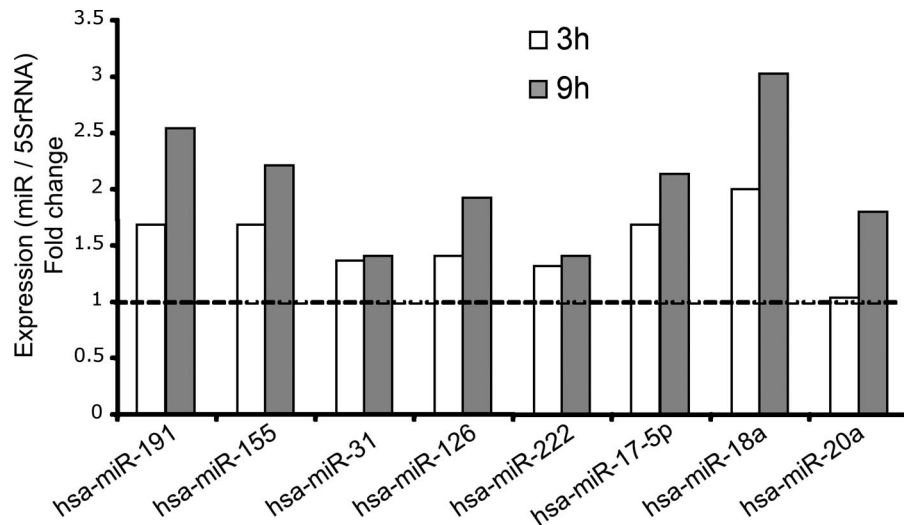


Fig. S6. Differential miRNA expression of hsa-miR-191, -155, -31, -126, -222, -17-5p, -18a, and -20a confirmed by qRT-PCR analysis. Data are expressed as fold-change from nontreated cells. 5SrRNA was used for normalization.

Other Supporting Information Files

[Table S1](#)